

8.1 Overview

- Medulloblastoma is an invasive, high-grade (WHO grade IV) embryonal tumor defined both by histologic grade and location in the cerebellum.
 - Even though this tumor shares histologic features with other central nervous system (CNS) embryonal tumors (primitive neuroectodermal tumors), it has been historically regarded as a distinct entity.
 - Recent molecular studies, including genomic and gene expression profiling as well as signaling pathway dysregulation and biologic studies, have now justified its historical clinical definition as a distinct clinicopathologic entity with predominant occurrence in children.
 - Most are sporadic.
 - They occur less frequently in the setting of hereditary syndromes. These include Turcot's syndrome, with germline mutation of the adenomatous polyposis coli (*APC*) gene, and Gorlin's syndrome, the nevoid basal cell carcinoma syndrome with germline mutation of the *PTCH* gene, seen in less than 2% of medulloblastomas.
- peak is seen at ages 35–40 years. Rarely, it may be congenital.
- Patients present with symptoms and signs of cerebellar dysfunction, including truncal and appendicular ataxia, and raised intracranial pressure due to obstruction of the fourth ventricle and CSF flow, with headache, vomiting, and progressive lethargy.

8.2 Clinical Features

- Medulloblastomas account for 20% of malignant CNS tumors in childhood, the second most common malignancy in childhood.
- Most tumors occur in children below the age of 20, with a peak between 5 and 8 years of age. A second but smaller

A.M. Adesina, M.D., Ph.D. (✉)
 Department of Pathology, Texas Children's Hospital, Baylor
 College of Medicine, One Baylor Plaza, RM 286A,
 Houston, TX 77030, USA
 e-mail: aadesina@bcm.tmc.edu

J.V. Hunter, M.B.B.S.
 Department of Radiology, Texas Children's Hospital,
 6621 Fannin Street, Houston, TX 77030, USA

8.3 Neuroimaging

- Early onset of calcification of the falx cerebri, tentorium cerebelli, and dura, with bridging of the sella turcica due to calcification of the diaphragma sellae is seen with CT scans in 60–80% of patients with Gorlin's syndrome (Fig. 8.1).
- Midline vermian mass lesions in children or lateral cerebellar hemispheric tumors in adults are typical.
- Characteristically, MRI shows a predominantly solid mass, hypointense or isointense with gray matter, with moderate diffuse, nonhomogenous enhancement (Figs. 8.2, 8.3, 8.4, 8.5, 8.6, and 8.7).
- There is often associated restricted diffusion consistent with a small-cell and densely cellular tumor (Figs. 8.2 and 8.6).
- MR spectroscopy shows marked elevation of choline with little, if any, NAA peak (Fig. 8.8A).
 - Elevation of the taurine peak may also be seen in medulloblastoma.
- The extensively nodular variant often seen in patients less than 1 year old may present with multiple, grapelike, enhancing nodular features (Fig. 8.8B and C).
- Diffuse leptomeningeal enhancement and thecal sac drop metastases, when present, are consistent with CSF dissemination and poorer prognosis (Figs. 8.9, 8.10, 8.11, 8.12, and 8.13).
- There is often evidence of mass effect, including severe dilatation of the third and lateral ventricles, transependymal CSF flow, and brainstem compression (Figs. 8.10 and 8.12).

Fig. 8.1 Axial CT scan of a patient with Gorlin's syndrome (also known as basal cell nevus syndrome) associated with medulloblastoma. Note the characteristic abnormal, heavy calcification outlining the free edge of the tentorium and the falx in this young child



Fig. 8.2 Axial T2-weighted MR image (A) and apparent diffusion coefficient (ADC) maps (B) demonstrating a heterogeneously hyperintense mass extending bilaterally to the cerebellopontine angles in a 27-month-old boy. There is restricted diffusion within the tumor, which was confirmed to be a medulloblastoma on histology

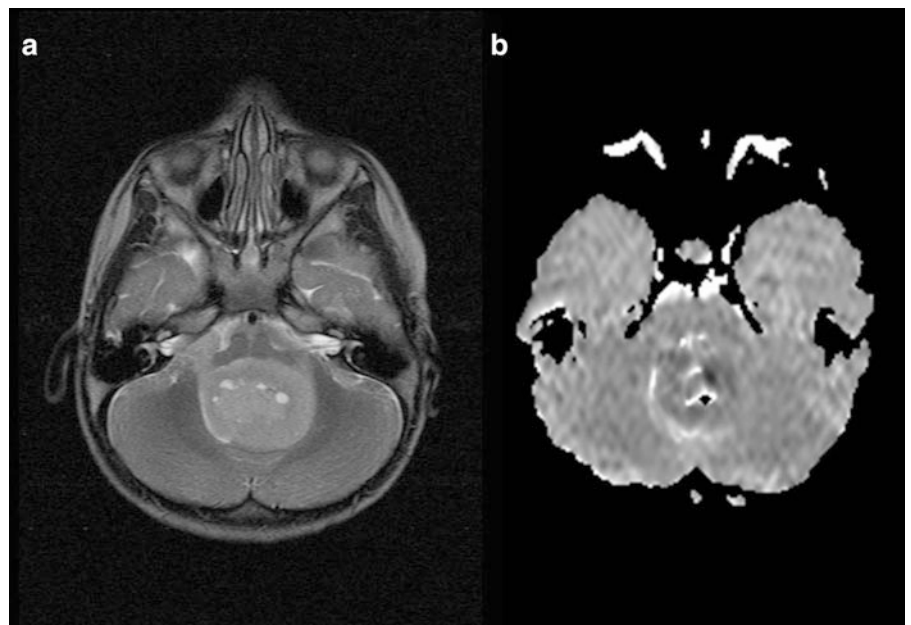


Fig. 8.3 Axial T1-weighted MR imaging before (A) and after (B) gadolinium demonstrates some central enhancement

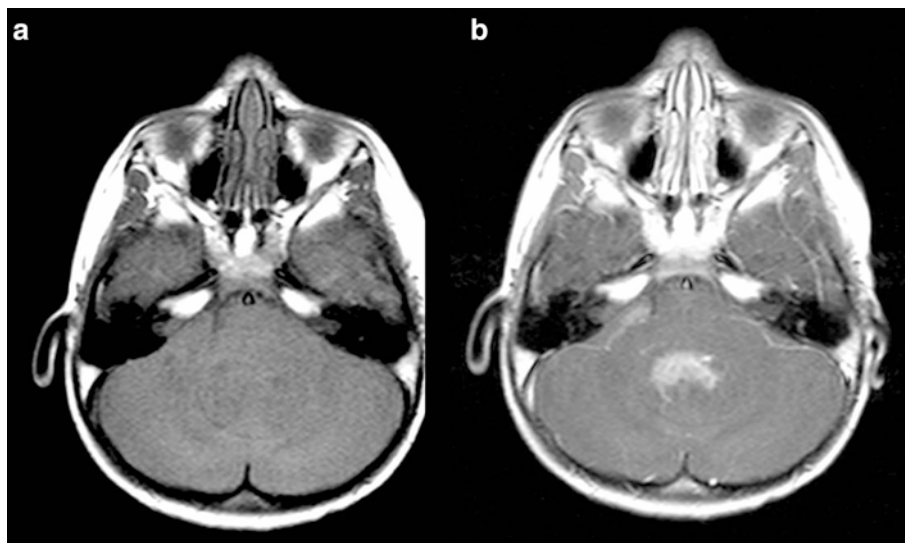


Fig. 8.4 Axial CT image showing hyperdense, centrally placed tumor within the posterior fossa, consistent with a highly cellular tumor such as a medulloblastoma or atypical teratoid/rhabdoid tumor (AT/RT)



Fig. 8.5 Sagittal T1-weighted image (A) and T2-weighted image (B) demonstrates a T1-hypointense and T2-hyperintense mass in the same patient as in Fig. 8.4

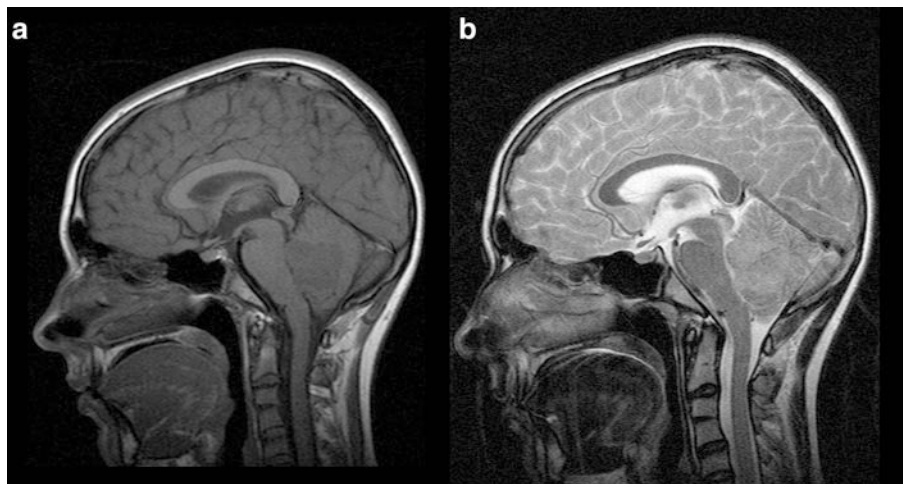


Fig. 8.6 (A, B) Diffusion-weighted imaging in the same patient as in Fig. 8.4 shows restriction as may be seen in a medulloblastoma, AT/RT or anaplastic ependymoma. This case was histologically proven to be a medulloblastoma

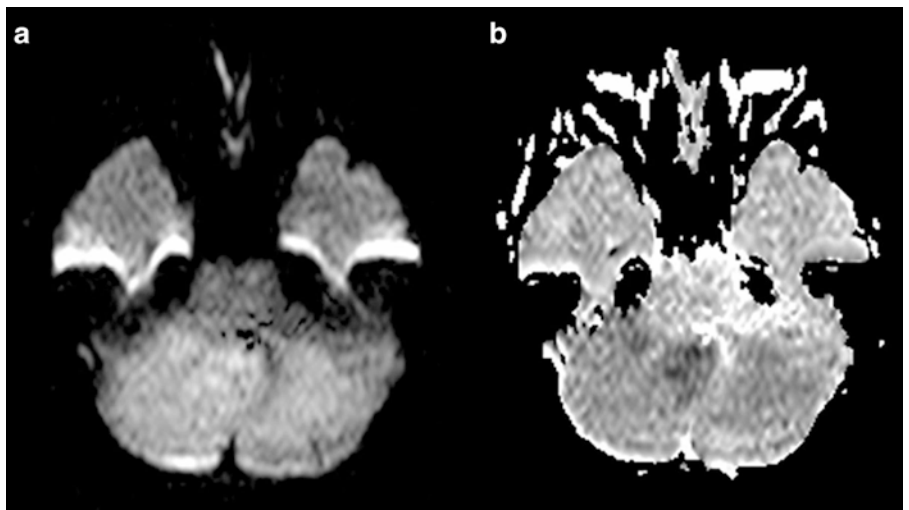


Fig. 8.7 T1-weighted axial (A) and sagittal (B) MR images following gadolinium administration, showing moderate enhancement, much less than would be seen with a solid pilocytic astrocytoma



8.4 Pathology

- Grossly, medulloblastoma presents commonly as a mid-line vermian mass (Fig. 8.14).
- Resection specimens or intraoperative biopsies are often soft, gray-pink, and appear necrotic. Extensively nodular or desmoplastic tumors may sometimes have a soft to slightly firm consistency with a lobulated appearance.
- *Intraoperative cytologic imprints or smears*
 - Moderate cellularity is characteristic. There is a good correlation between cytologic features and histologic classification as classic or nodular, anaplastic, or large cell medulloblastomas.
 - **Classic and nodular medulloblastomas** demonstrate monolayered sheets of relatively uniform, round to oval (occasionally elongated or carrot-shaped) molded nuclei with hyperchromasia and some chromatin clumping (Fig. 8.15A). Molded, markedly atypical cells with high nucleocytoplasmic ratio in CSF cytopspin are consistent with dissemination (Fig. 8.15B). Rosette-like arrangements representing Homer Wright rosettes may be seen (Fig. 8.16).
 - **Anaplastic medulloblastomas** demonstrate a significant component of large, pleomorphic cells with prominent chromatin clumping and visible nucleoli. “Cell wrapping” or “cannibalism” (the nucleus of one cell wrapped around the nucleus of another) and apoptotic nuclei are frequent (Fig. 8.17). Occasional multinucleated cells may sometimes be seen.
 - **Large cell medulloblastoma**, when present or predominant, often shows a discohesive, monotonous population of large cells with open chromatin and visible nucleoli, sometimes mimicking the cytologic monotony of large cell lymphomas (Fig. 8.18).
- Endothelial proliferation and mitosis may be present in all cytologic types.
- Rare evidence of cytologic differentiation with astrocytic, ganglionic, or melanocytic differentiation (with melanin pigments), or rhabdomyoblastic differentiation (strap cells) may be seen.
- *Histology*: Varied histologic features may be seen between and within tumors.
 - **Classic medulloblastomas** are composed of monotonous sheets of small cells (Fig. 8.19).
 - Slight nuclear irregularity is often present.
 - Mitoses are present but often variable.
 - Necrosis may be present, with or without pseudopalisading.
 - Apoptosis is often present.
 - Endothelial proliferation is present and sometimes can be florid.
 - Neuroblastic differentiation is seen as the Homer Wright rosette (Fig. 8.20).
 - Mature neuronal differentiation as ganglion or “ganglioid” cells may be seen but must be distinguished from entrapped neurons.
 - A spindle or fascicular pattern, when present, is usually focal (Fig. 8.21)
 - Prominent nuclear irregularity with nucleoli and pleomorphism suggests the presence of anaplastic features, which may be focal; a transition from classic to anaplastic may be appreciable (Fig. 8.22). Extensive anaplasia may justify designation as an **anaplastic subtype**.
 - Anaplasia may vary from slight to moderate to severe (Figs. 8.23 and 8.24).

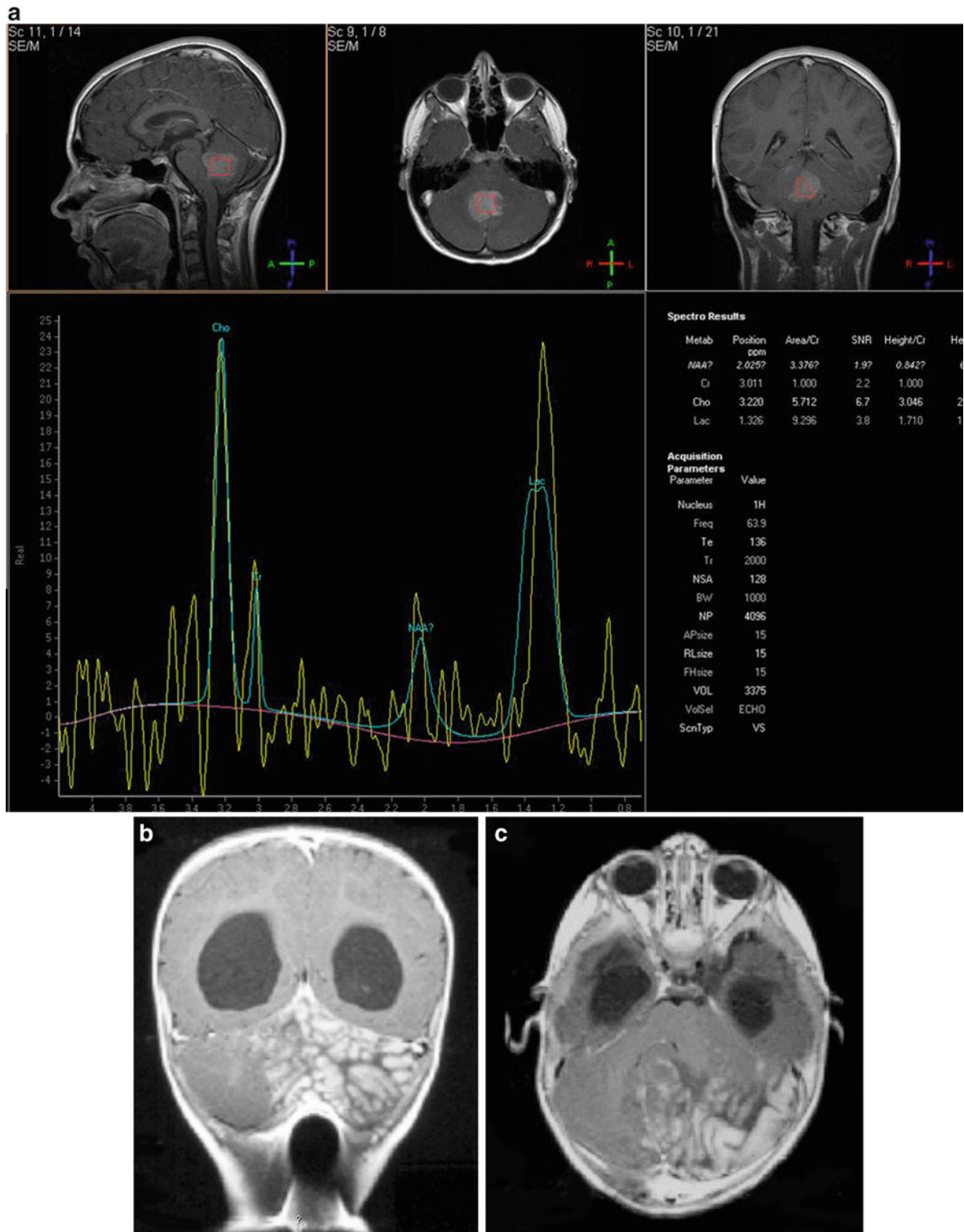


Fig. 8.8 (A) Typical appearances of MR spectroscopy utilizing a long TE in the same patient as in Fig. 8.7, demonstrating a marked decrease in N-acetyl aspartase (NAA), a marker of neuronal and axonal integrity, and a significant elevation in choline, a marker of cell membrane turn-

over. Also present is a lipid peak consistent with the presence of necrosis. (B, C) Coronal and axial T1-weighted post-gadolinium MR images show a cerebellar mass with grapelike nodules in a patient with an extensively nodular medulloblastoma



Fig. 8.9 Sagittal T1-weighted, post-gadolinium imaging of the lumbosacral spine in a patient with medulloblastoma, demonstrating evidence for abnormal leptomeningeal enhancement in the dorsal surface of the thoracic cord, as well as evidence for extensive drop metastases within the distal thecal sac

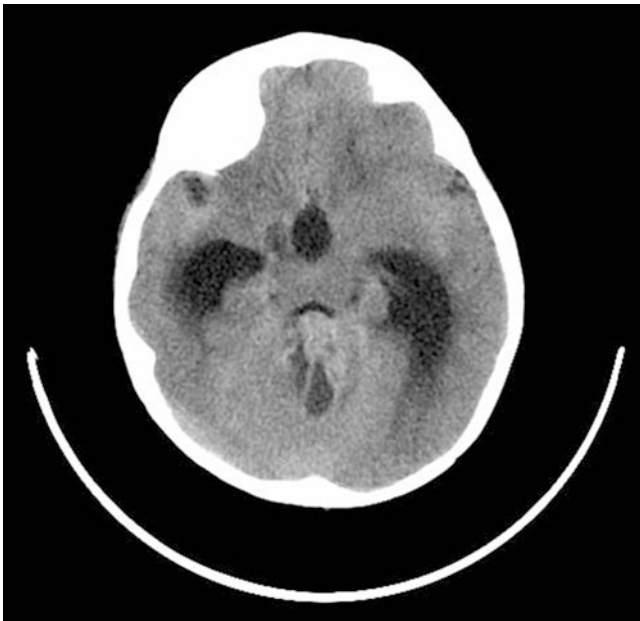


Fig. 8.10 Unenhanced axial CT scan demonstrating a mixed solid and cystic tumor arising in the posterior fossa and causing obstruction to the supratentorial ventricular system. The solid portion of the tumor appears hyperdense, consistent with high cellularity. Note also the high density outlining the Sylvian fissures, suspicious for disseminated tumor

- Regions with monomorphic, discohesive, large round cells with prominent nucleoli are suggestive of the presence of a **large cell component** (Fig. 8.25).
 - Predominance of large cells or severe anaplasia represents the large cell or anaplastic subtype and accounts for about 4% of medulloblastoma.
 - Severe anaplasia is often associated with increased apoptosis, increased frequency of mitotic activity, and cell wrapping or cannibalism.
- **Nodular (desmoplastic) medulloblastoma** is characterized by the presence of multiple reticulin-free, pale nodules of neurocytic cells within a neuropil-like background, which are rarely mitotic with increased apoptosis (Figs. 8.26, 8.27, and 8.28).
 - Leptomeningeal invasion with florid, reactive desmoplasia (collagenous fibrosis), often demonstrating medium- to large-sized leptomeningeal vessels, may occur but does not constitute a desmoplastic medulloblastoma (Fig. 8.29).
 - Internodular areas are reticulin-rich and are composed of cells similar to those of classic medulloblastoma.
- These areas tend to exhibit more brisk mitotic activity than is seen within the pale nodules.
 - Internodular areas may sometimes show varying degrees of anaplasia (see Fig. 8.23).
- The **extensively nodular medulloblastoma** (previously termed *cerebellar neuroblastoma*) is a variant showing florid nodularity and neurocytic differentiation with an absent or minimal undifferentiated internodular component.
 - Cells are often arranged in a streaming pattern within a fibrillary matrix (Figs. 8.30 and 8.31).
 - Ganglion cell differentiation (forming cerebellar ganglioneuroblastoma) also may be present (Fig. 8.32).
- **Biphasic medulloblastoma** represents a tumor with mixed classic and nodular components, in which the nodular component is not surrounded by desmoplasia; that is, the internodular areas are reticulin-free. This distinction from the nodular/desmoplastic medulloblastoma is important.
- **Infrequent patterns of differentiation** include:
 - Astrocytic differentiation, which must be distinguished from entrapped reactive astrocytes (Figs. 8.33 and 8.34).
 - Skeletal muscle or rhabdomyoblastic differentiation may rarely be seen as strap cells with or without striations; this pattern constitutes the medulloblastoma with myogenic differentiation (synonym: **medullomyoblastoma**) (Fig. 8.35).
 - Melanocytic differentiation with melanin pigment production constitutes the rare medulloblastoma with melanotic differentiation (synonym: **melanotic medulloblastoma**) (Fig. 8.36).
 - Premelanosomes and melanosomes are demonstrable by electron microscopy.

Fig. 8.11 (A) Restricted diffusion demonstrated within the enhancing solid portion of this tumor on an ADC map suggests a medulloblastoma, AT/RT, or anaplastic ependymoma in the differential diagnosis. (B) Note the presence of abnormal leptomenigeal enhancement in the axial T1-weighted, postcontrast image

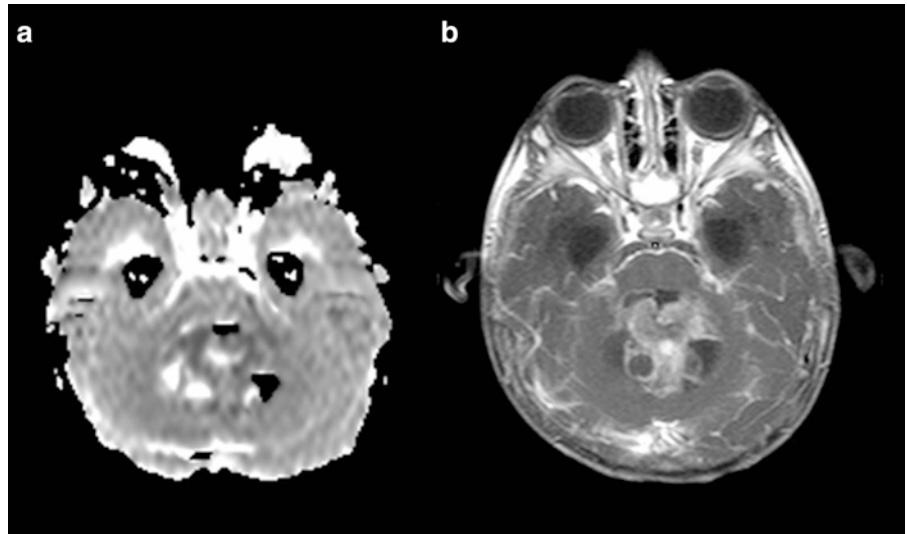


Fig. 8.12 Sagittal (A) and coronal (B) T1-weighted images from the same patient as in Fig. 8.11, following the administration of gadolinium. Florid, abnormal leptomenigeal enhancement is observed with hydrocephalus and extension of abnormal enhancement into the spinal canal. Histology revealed a medulloblastoma in this 15-month-old boy

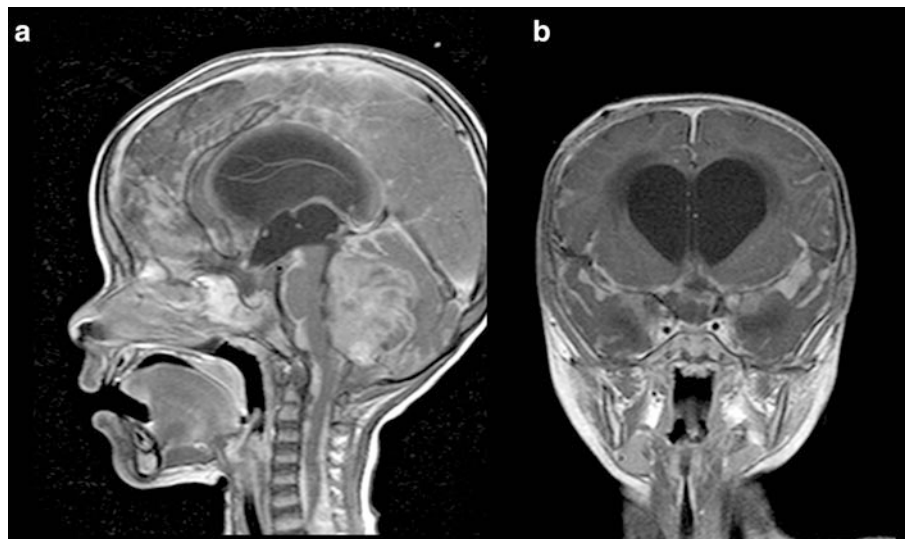


Fig. 8.13 (A, B) MR images of the spine, demonstrating extensive abnormal, thick leptomenigeal enhancement surrounding the entire spinal cord at the time of presentation

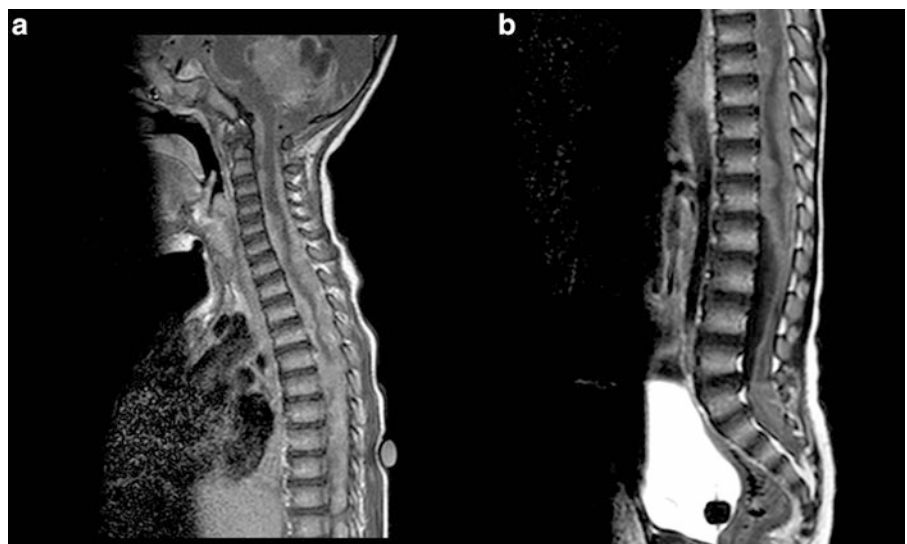


Fig. 8.14 Medulloblastoma arising in the vermis, with associated necrosis and hemorrhage

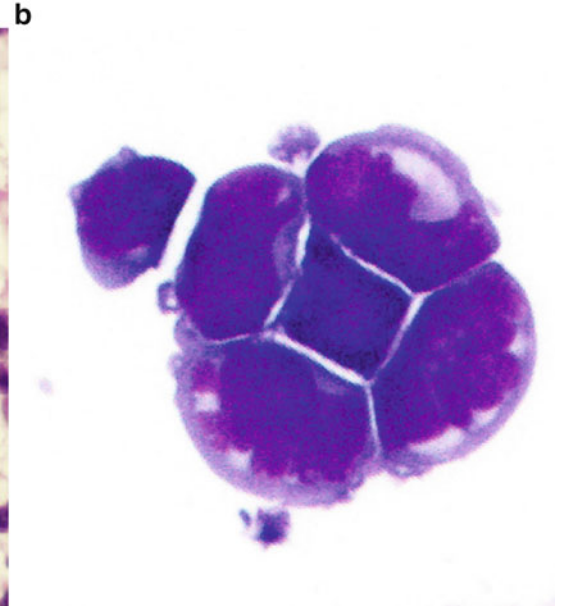
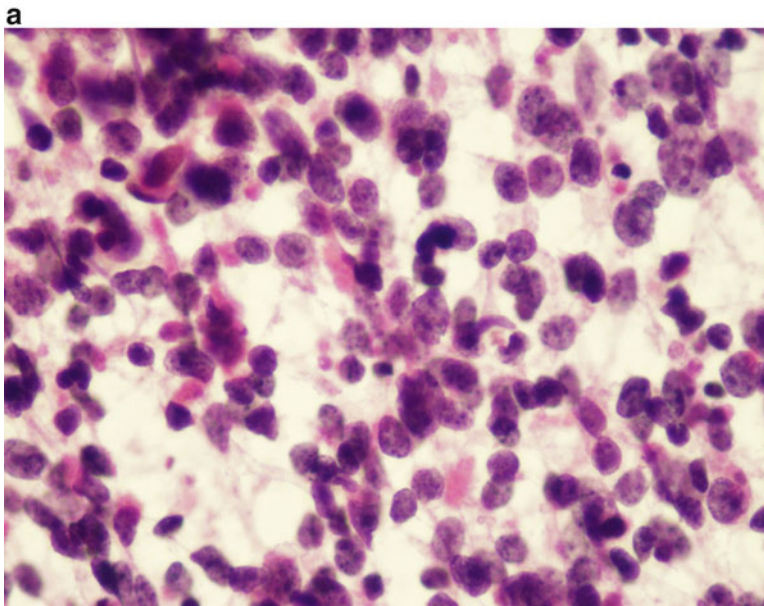
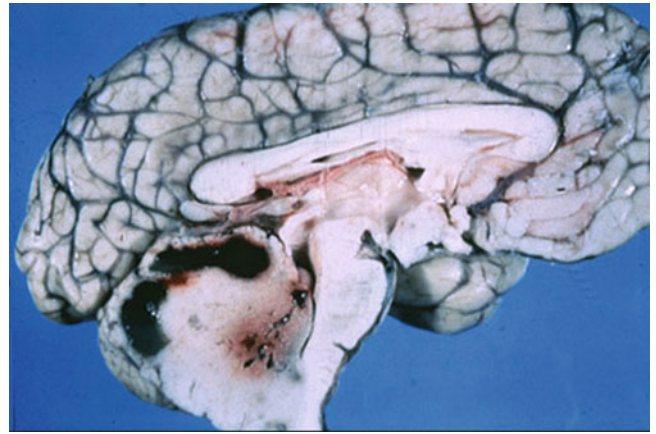


Fig. 8.15 Intraoperative cytology preparation of a classic medulloblastoma, showing "small blue cells" with limited cytoplasm, moderate cellular pleomorphism, and nuclei with chromatin condensation and micronucleoli (A). Note the lack of a fibrillary background and an occasional apoptotic body.

CSF from a patient with medulloblastoma (B) shows a cluster of disseminated malignant cells, cellular molding, irregular nuclear contour, and high nucleocytoplasmic ratio

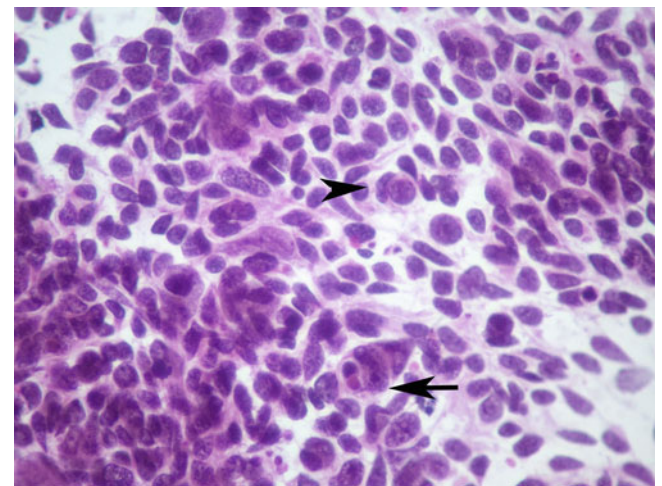
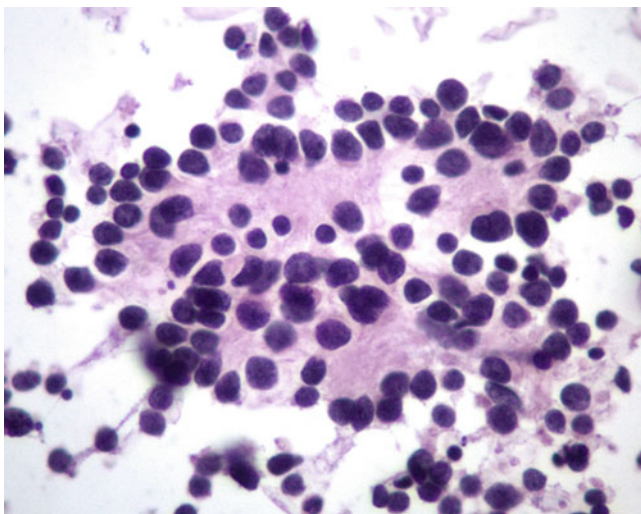


Fig. 8.16 Cytology preparation showing Homer Wright rosettes

Fig. 8.17 Cytology preparation of an anaplastic medulloblastoma showing carrot-shaped cells, moderate cellular pleomorphism, "cell wrapping" (arrowhead), "cannibalism" (arrow), and hyperchromatic nuclei with chromatin condensation and micronucleoli

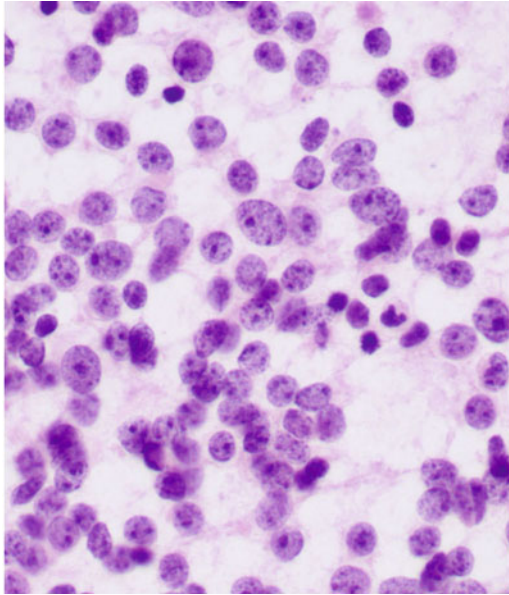


Fig. 8.18 Cytology preparation of a large cell medulloblastoma showing a monomorphic cytology, nuclei with open chromatin, and slightly prominent micronucleoli

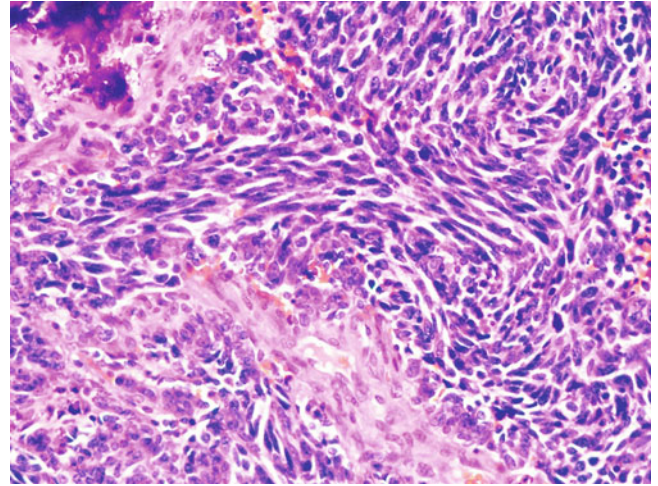


Fig. 8.21 Spindled and fascicular pattern of growth in a classic medulloblastoma

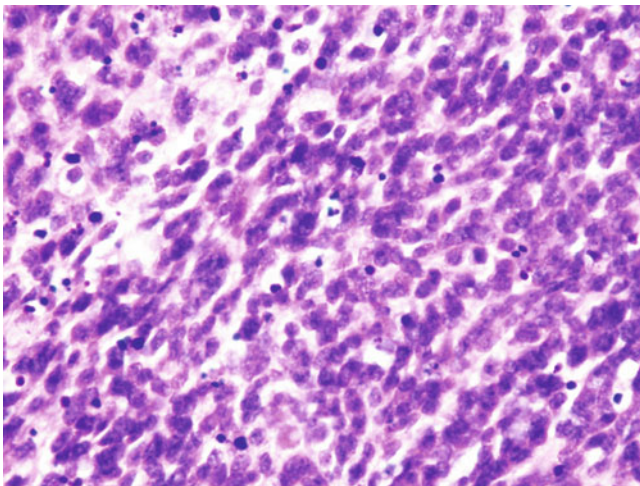


Fig. 8.19 Classic medulloblastoma with high cellularity and overlapping nuclei, some of which are carrot-shaped. A few "dark" apoptotic bodies are present

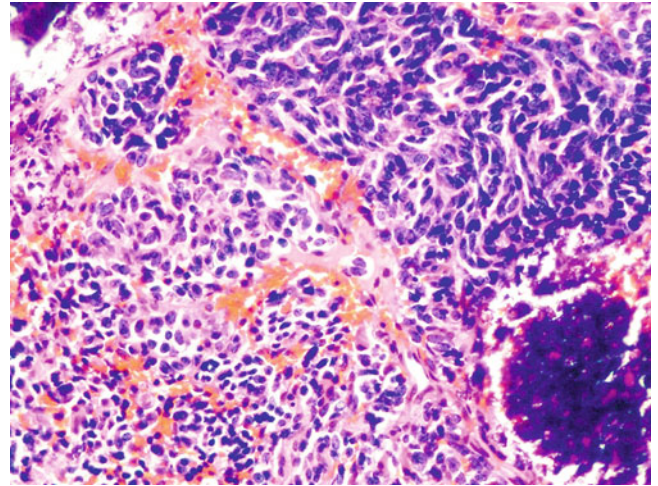


Fig. 8.22 Transition from classic medulloblastoma (*left bottom*) to low-grade anaplastic features (*right top*)

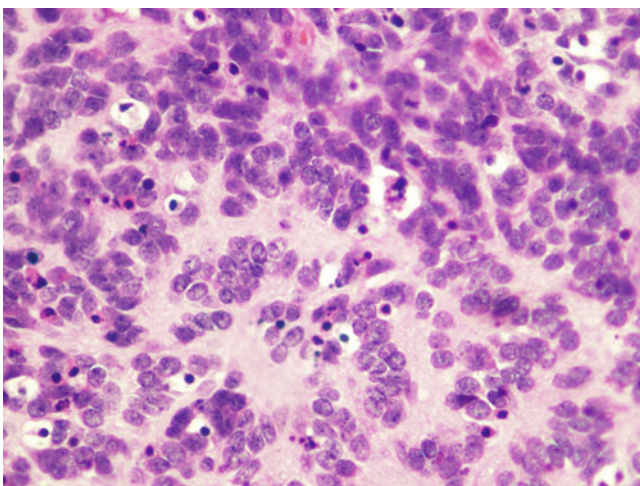


Fig. 8.20 Classic medulloblastoma with Homer Wright rosettes

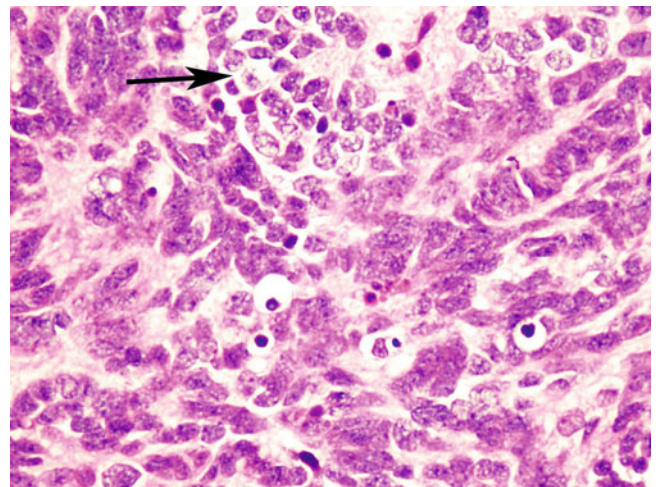


Fig. 8.23 Progressive transformation of internodular areas with increasing anaplasia is sometimes seen in desmoplastic medulloblastoma. A residual pale nodule area is shown partially at the top of the image (*arrow*)

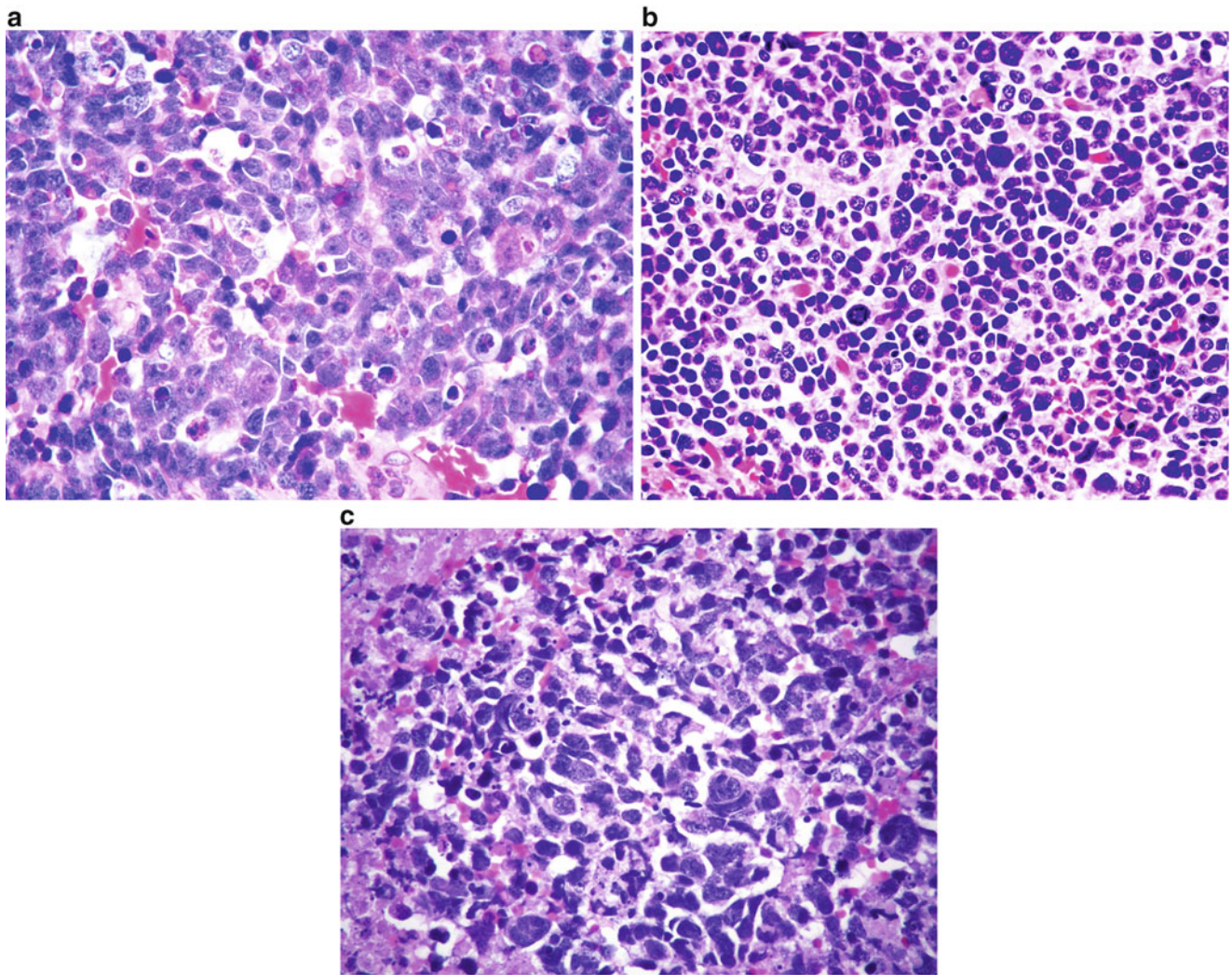
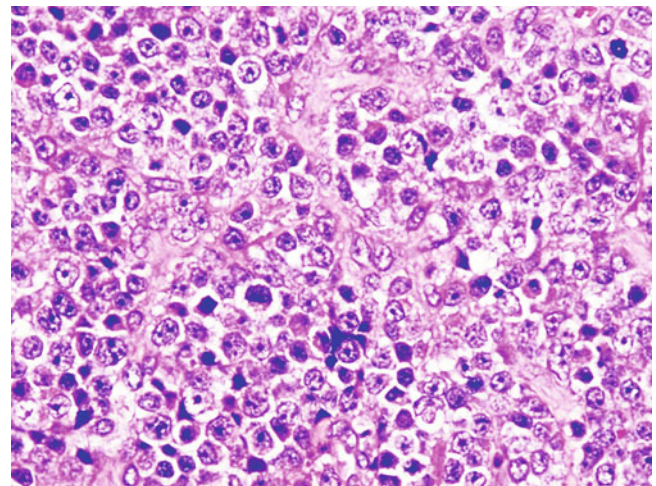


Fig. 8.24 (A–C) Anaplastic medulloblastoma with severe anaplasia. Note variable patterns of marked cellular pleomorphism, florid apoptosis, karyorrhexis, and frequent cell wrapping and cannibalism

Fig. 8.25 Large cell medulloblastoma showing cellular monomorphism, vesicular nuclei, and distinct nucleoli. Note the similarity of this morphology to that of a diffuse large cell lymphoma



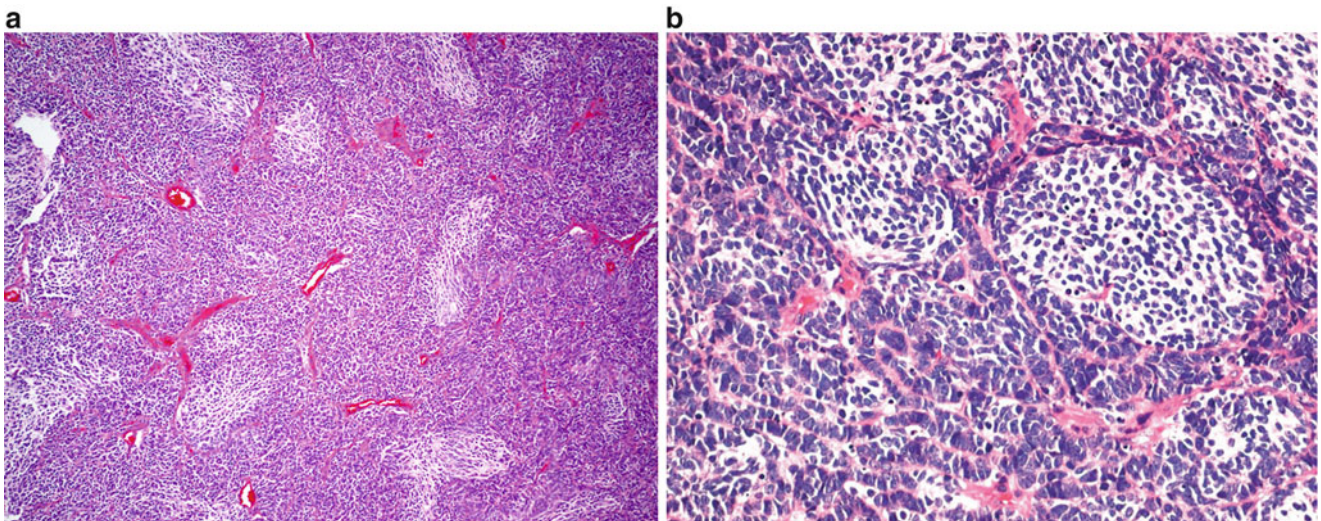


Fig. 8.26 Low-magnification (A) and higher-magnification (B) views of a desmoplastic (nodular) medulloblastoma, showing the characteristic pale nodules

Fig. 8.27 Desmoplastic (nodular) medulloblastoma showing pale nodules (left), which are composed of neurocytes in a more differentiated, fibrillary, neuropil-like background. Contrast with the less-differentiated neuroblastic internodular region (right)

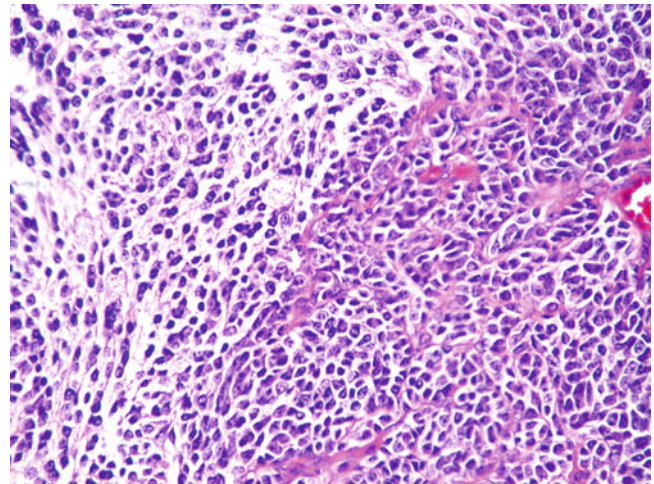
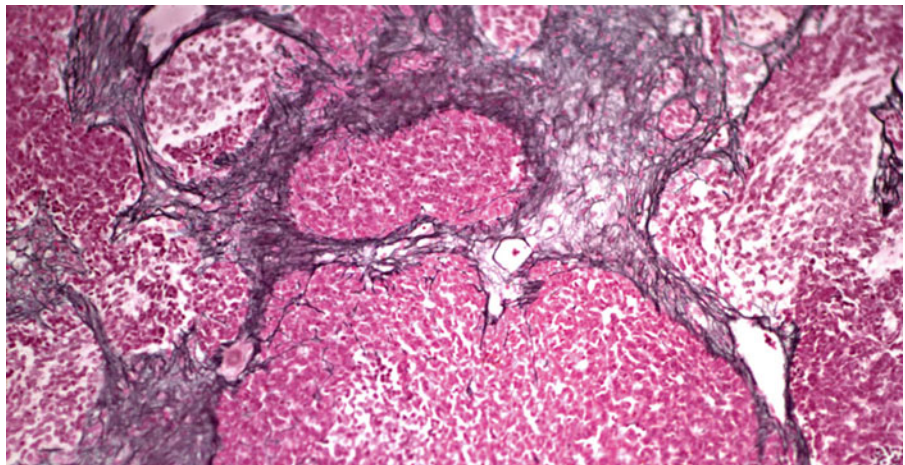


Fig. 8.28 Desmoplastic (nodular) medulloblastoma showing reticulin-free pale nodules and reticulin-positive internodular areas



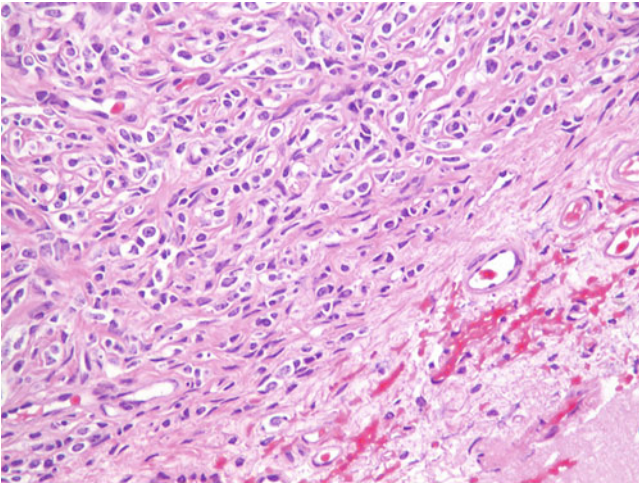


Fig. 8.29 Fibrosis following leptomeningeal invasion in a medulloblastoma. This should not be equated with a desmoplastic (nodular) medulloblastoma

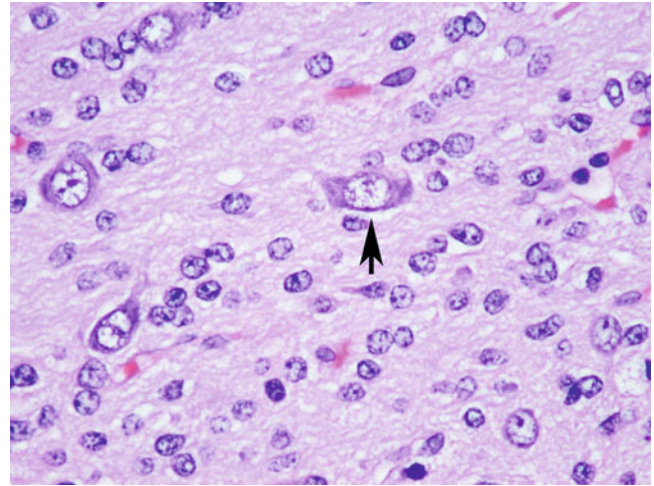


Fig. 8.32 Neuronal/ganglionic (arrow) differentiation in a medulloblastoma

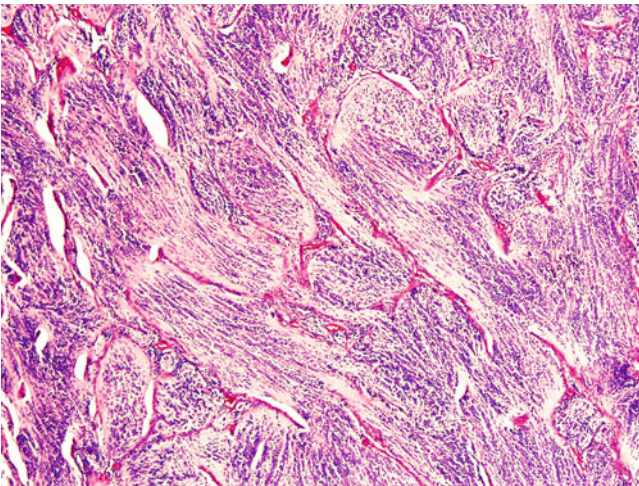


Fig. 8.30 Extensively nodular medulloblastoma composed of interlacing fascicles of differentiated neurocytes in a “fibrillary” neuropil-like matrix with limited internodular areas

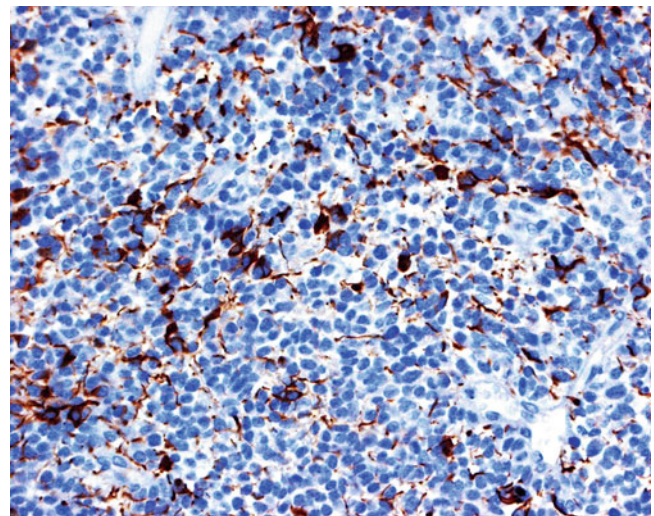


Fig. 8.33 Astrocytic differentiation in a medulloblastoma demonstrated by reactivity with antibody for glial fibrillary acidic protein (GFAP) in a subpopulation of tumor cells

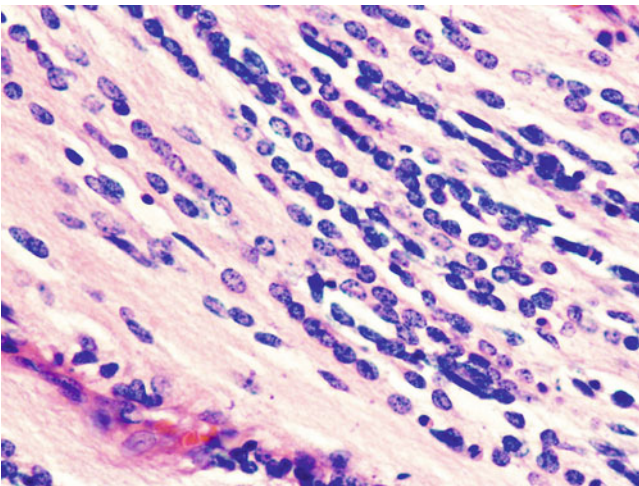


Fig. 8.31 Extensively nodular medulloblastoma with neurocytes arranged in rows reminiscent of an “Indian file” pattern

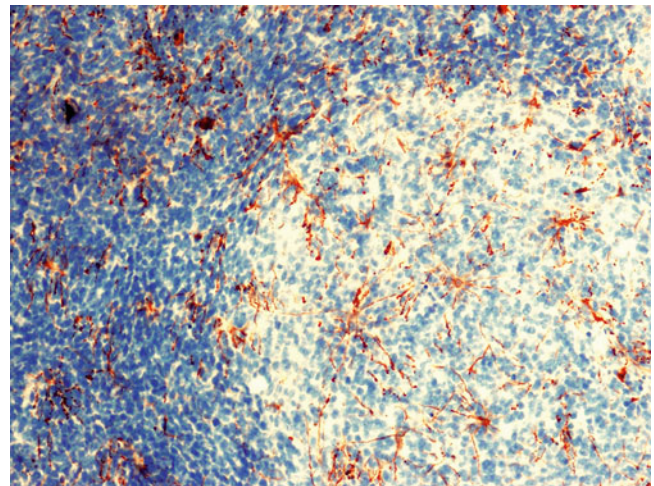


Fig. 8.34 Nonneoplastic reactive astrocytes within a medulloblastoma showing immunoreactivity for GFAP

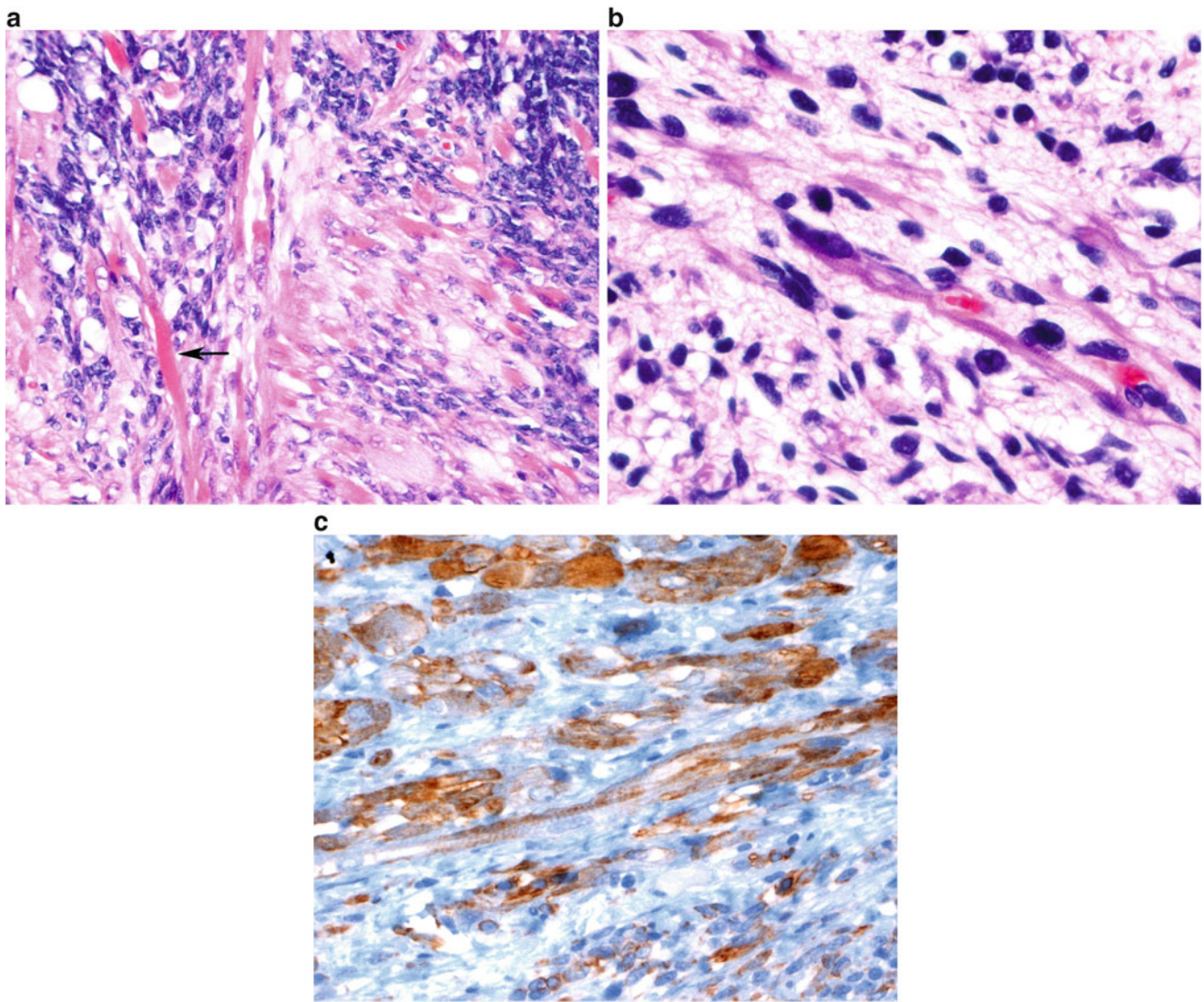
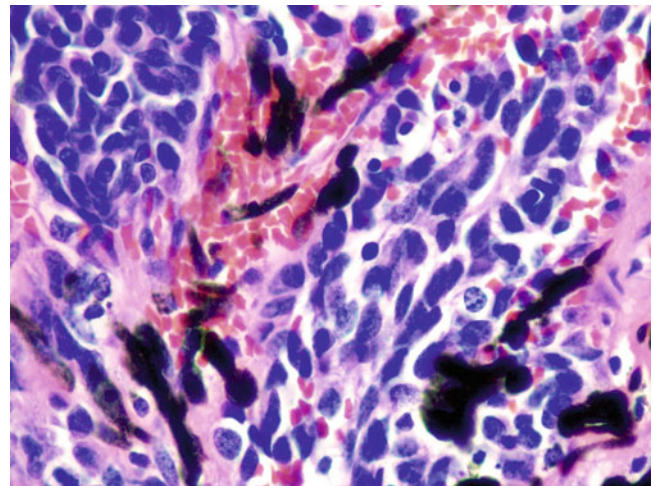


Fig. 8.35 Medullomyoblastoma with florid skeletal muscle differentiation (*arrow*) (A), demonstrable strap cells with cross-striations (B), and desmin immunoreactivity in tumor cells (C)

Fig. 8.36 Melanotic differentiation in a medulloblastoma



8.5 Immunohistochemistry

- Medulloblastomas show diffuse immunopositivity for synaptophysin (Fig. 8.37) and variable immunopositivity for chromogranin, neurofilament protein, and the neuronal marker NeuN.
- Glial fibrillary acidic protein (GFAP) often highlights trapped reactive astrocytes. Rare positivity of tumor cells is seen (*see* Figs. 8.33 and 8.34).
- Immunopositivity for retinal S-antigen and rhodopsin may be rarely seen in tumors with photoreceptor differentiation.
- Epithelial membrane antigen (EMA) is usually negative.
- *p53* immunopositivity is seen in a subset of medulloblastomas. An increased proportion of positive cells often correlates with increasing anaplasia and poorer survival (Fig. 8.38).
- The MIB-1 (proliferation) index is variable, often very high (30–80 %) (Fig. 8.39).

8.6 Electron Microscopy

- Electron microscopy shows tumor cells (often paucicellular) in organelles but with demonstrable neurosecretory granules.
- Cellular processes are frequent and contain microtubules.
- Synaptic-type junctions may be seen.

8.7 Molecular Pathology

- Medulloblastomas are presumed to arise from precursor stem cells in the external granular layer for lateral hemispheric nodular or desmoplastic medulloblastomas, and from dysplastic precursor cells arrested during migration for other vermian variants.

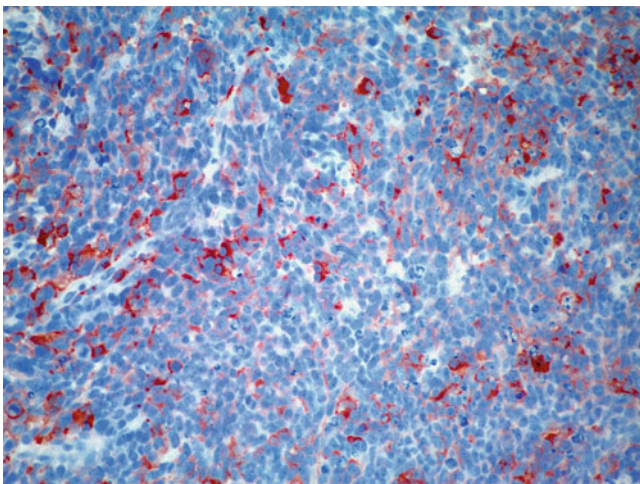


Fig. 8.37 Immunoreactivity for synaptophysin is consistent with neuroblastic differentiation in this poorly differentiated embryonal tumor

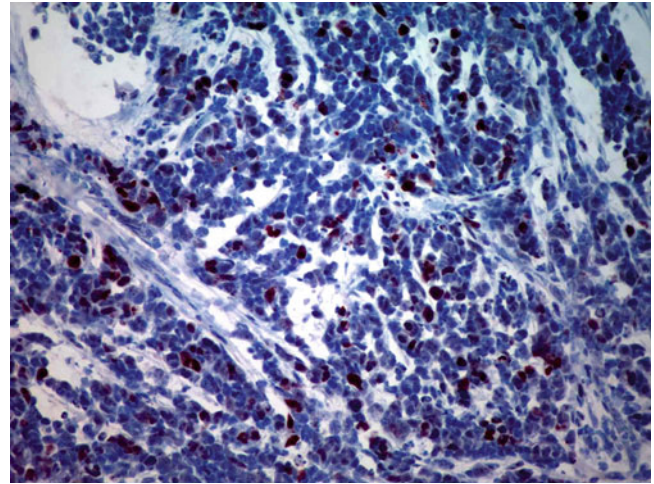


Fig. 8.38 A subpopulation of tumor cells exhibit immunoreactivity of p53 protein, consistent with dysregulation of p53 in this tumor and implication of a poor prognosis

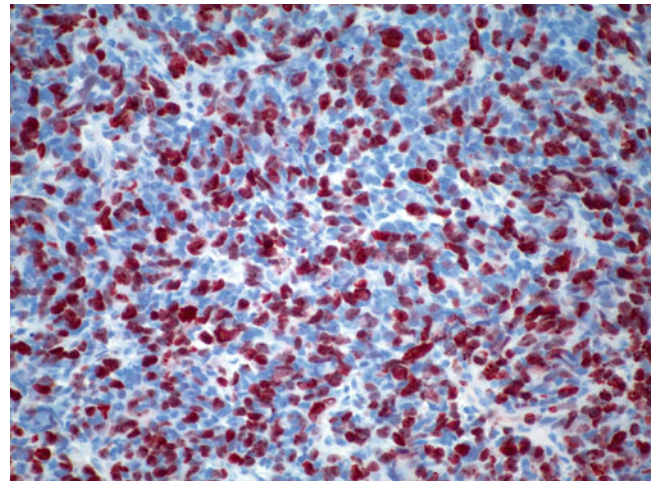


Fig. 8.39 Ki-67 immunoreactivity showing a high proliferation index

- Using gene expression profiling, medulloblastomas are molecularly classified into four groups:
 - Group A with *wnt* pathway activation
 - Group B with *SHH* pathway activation
 - Groups C and D, collectively referred to as non A/non B. Non A/non B classification is often associated with aggressive histology, *MYC* amplification, and poor prognosis.
- Activation of the *wnt* signaling pathway through mutation of the *APC* gene has been associated with Turcot syndrome and only 3–4 % of sporadic medulloblastoma.
- *Wnt* pathway-activated tumors account for about 10 % of medulloblastomas and show demonstrable nuclear localization for *beta catenin* and/or monosomy 6. *DDX3X* gene mutation is also seen in 50 % of *wnt* pathway tumors.

- *PTCH* gene loss of function mutation, as well as mutations of *SMO*, *SUFU*, and *Gli2* result in the activation of the sonic hedgehog (*SHH*) signaling pathway in 30% of medulloblastomas.
- *SHH* pathway activation is seen classically in nodular or desmoplastic medulloblastoma. *Gli1* and *Gli2*, representing downstream effectors of *SHH* pathway activation, are also often demonstrable in up to 85% of medulloblastomas. The proportion of tumors classified as *SHH* molecular subgroup drops significantly when classified based on the expression of *GAB1*, *filamin A*, and/or *YAP1*. *SHH*-activated tumors with p53 mutation carry a significantly poor prognosis.
- Amplification of *MYCC* and less commonly *MYCN* is a common finding in large cell/anaplastic medulloblastoma (Figs. 8.40 and 8.41); *MYCC* amplification is frequently associated with Group C, and *MYCN* amplification, with group D.
- Gains of *CDK6* (7q21), *hTERT* (5p15), *OTX2* (14q22) (more frequently seen in group C), and *FoxG1* (14q12) have been reported.
- 17p deletion with isochromosome 17q is the commonest cytogenetic abnormality in medulloblastoma, present in 30–40% of tumors (Fig. 8.42); it is seen particularly in group D tumors. Potential target genes in the 17p deletion include *HIC1* (17p13.3), frequently hypermethylated in medulloblastoma, and *REN* (17p13.2), a negative regulator of the *SHH* signaling pathway.
- Losses of 16q, 10q, and 11q are present in a subset of the tumors.
- Increased activation of the *Notch* signaling pathway; overexpression of *PAX5*, *PAX6* and *SOX4*; and overexpression of repressors of neural differentiation *REST* and *FoxG1* have all been reported in medulloblastoma.

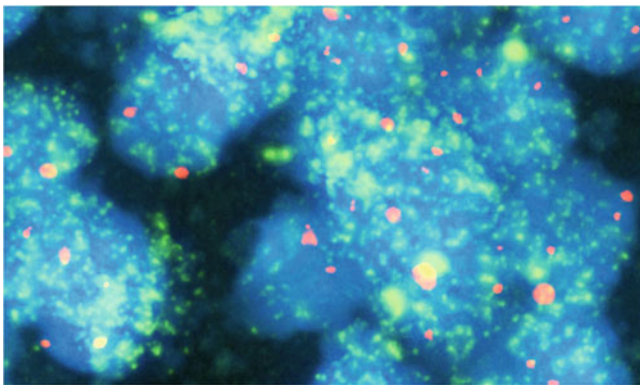


Fig. 8.40 Fluorescence in situ hybridization (FISH) using an *MYCN*-specific probe demonstrates gene amplification (*green*) in an anaplastic medulloblastoma. The chromosome 2 centromeric reference probe is *red*

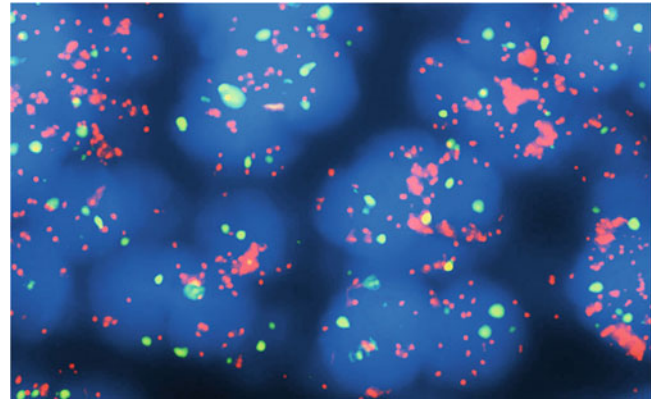
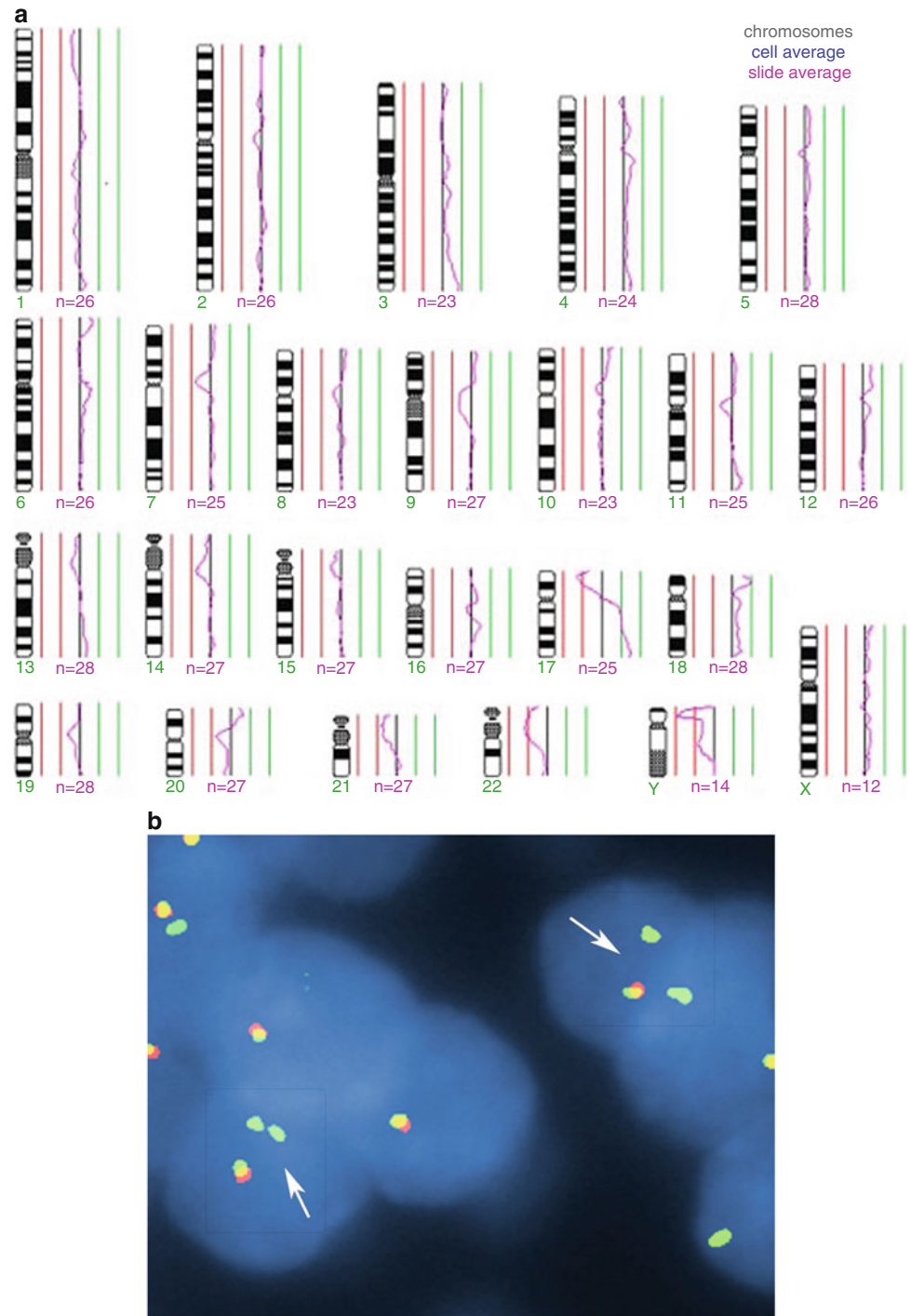


Fig. 8.41 FISH using a *c-myc*-specific probe demonstrates gene amplification (*red*) in an anaplastic medulloblastoma. The chromosome 8 centromeric reference probe is *green*

8.8 Differential Diagnosis

- Medulloblastomas may have areas with prominent perivascular pseudorosettes, thus raising anaplastic ependymoma as a major differential diagnosis.
 - Ependymomas tend to show variation in cellularity, however, including regions of well-differentiated ependymoma.
 - EMA is often positive in ependymomas and negative in medulloblastoma.
 - Synaptophysin is positive in perivascular pseudorosettes of medulloblastoma, whereas GFAP staining is more characteristic of ependymoma.
 - Nuclear positivity for NeuN is not helpful, as it may be positive in both tumor types.
- Atypical teratoid /rhabdoid tumor (AT/RT) may have a prominent PNET-like small round cell component, whereas large cell or anaplastic medulloblastoma may mimic AT/RT.
 - FISH with *INI-1* locus-specific probe shows no demonstrable allelic deletion in medulloblastoma.
 - Similarly, immunostain with BAF-47 (anti-*INI1*) antibody shows positive nuclear staining in the neoplastic cells in medulloblastoma but negative staining in AT/RT.
- Medulloblastoma needs to also be differentiated from small cell glioblastoma.
 - Small cell glioblastoma will characteristically show widespread GFAP positivity and lack evidence of neural differentiation (presence of Homer Wright rosettes or neuronal immunohistochemical markers typical of medulloblastoma).

Fig. 8.42 (A)
 Conventional comparative genomic hybridization (CGH) analysis demonstrating loss of 17p and gain of 17q. **(B)** FISH analysis showing one copy of 17p (red probe signal) and three copies of 17q (green probe signal), consistent with cytogenetic findings of isochromosome 17q



- Other small round blue cell tumors of children metastatic to the CNS (rhabdomyosarcoma, Ewing sarcoma, leukemia/lymphoma, etc.) can all be effectively differentiated from medulloblastoma by immunohistochemistry.
- Metastatic neuroblastoma may closely mimic medulloblastoma, but it would be unlikely for neuroblastoma to present solely as a CNS metastasis without the primary peripheral lesion having been identified by imaging studies or a previous biopsy.

8.9 Prognosis

- The following clinical characteristics define high-risk patients:
 - Age less than 3 years.
 - Postresection residual tumor larger than 1.5 cm.
 - Metastatic disease at presentation with Chang stages M1–4.
- Large cell and anaplastic histology are associated with poor survival.
- Poor prognostic molecular markers include amplification of *MYCC* or *MYCN* and overexpression of *c-erbB2* or *p53*.
- The nodular/desmoplastic and the extensively nodular phenotypes are associated with favorable outcome and better survival than the classic medulloblastoma.
- *Wnt* pathway activation with nuclear expression of β -catenin and/or monosomy 6 has been reported as a good prognostic marker.

Suggested Reading

- Adesina AM, Veo BL, Courteau G, Mehta V, Wu X, Pang K, et al. FOXG1 expression shows correlation with neuronal differentiation in cerebellar development, aggressive phenotype in medulloblastomas, and survival in a xenograft model of medulloblastoma. *Hum Pathol.* 2015;46:1859–71.
- Bailey P, Cushing H. Medulloblastoma cerebelli: a common type of mid-cerebellar glioma of childhood. *Arch Neurol Psychiatry.* 1925;14:192–224.
- Ellison DW, Dalton J, Kocak M, Nicholson SL, Fraga C, Neale G, et al. Medulloblastoma: clinicopathological correlates of SHH, WNT, and non-SHH/WNT molecular subgroups. *Acta Neuropathol.* 2011;121:381–96.
- Giangaspero F, Rigobello L, Badiali M, Loda M, Andreini L, Basso G, et al. Large cell medulloblastoma. A distinct variant with highly aggressive behavior. *Am J Surg Pathol.* 1992;16:687–93.
- Giangaspero F, Perilongo G, Fondelli MP, Brisigotti M, Carollo C, Burnelli R, et al. Medulloblastoma with extensive nodularity: a variant with favorable prognosis. *J Neurosurg.* 1999;91:971–7.
- Giangaspero F, Wellek S, Masuoka J, Gessi M, Kleihues P, Ohgaki H. Stratification on the basis of histopathologic grading. *Acta Neuropathol.* 2006;112:5–12.
- Helton KJ, Fouladi M, Boop FA, Perry A, Dalton J, Kun L, Fuller C. Medulloblastoma: a radiographic and clinicopathologic analysis of six cases and review of the literature. *Cancer.* 2004;101:1445–54.
- Louis DN, Perry A, Reifenberger G, von Deimling A, Figarella-Branger D, Cavenee WK, Ohgaki H, Wiestler OD, Kleihues P, Ellison DW. The 2016 World Health Organization classification of tumors of the central nervous system: a summary. *Acta Neuropathol.* 2016;131:803–20.
- Louis DN, Ohgaki H, Wiestler OD, Cavenee WK, editors. WHO classification of tumours of the central nervous system. Lyon: International Agency for Research on Cancer (IARC); 2016.
- Meyers SP, Kemp SS, Tarr RW. MR imaging features of medulloblastomas. *AJR Am J Roentgenol.* 1992;158:859–65.
- Northcott PA, Korshunov A, Witt H, Hielscher T, Eberhart CG, Mack S, et al. Medulloblastoma comprises four distinct molecular variants. *J Clin Oncol.* 2011;29:1408–14.
- Panigrahy A, Krieger MD, Gonzalez-Gomez I, Liu X, McComb JG, Finlay JL, et al. Quantitative short echo time 1H-MR spectroscopy of untreated pediatric brain tumors: preoperative diagnosis and characterization. *AJNR Am J Neuroradiol.* 2006;27:560–72.
- Taylor MD, Northcott PA, Korshunov A, Remke M, Cho YJ, Clifford SC, et al. Molecular subgroups of medulloblastoma: the current consensus. *Acta Neuropathol.* 2012;123:465–72.